Available online at www.sciencedirect.com
ScienceDirect
Cement and Concrete Research 38 (2008) 848–860
Cement and Concrete Research

Influence of limestone on the hydration of Portland cements

Barbara Lothenbach [a,*], Gwenn Le Saout [b], Emmanuel Gallucci [b], Karen Scrivener [b]

[a] Empa, Laboratory for Concrete & Construction Chemistry, Überlandstrasse 129, CH-8600 Dübendorf, Switzerland
[b] EPFL, Laboratory of Construction Materials, station 12, CH-1015 Lausanne, Switzerland

Received 12 September 2007; accepted 8 January 2008

Abstract

The influence of the presence of limestone on the hydration of Portland cement was investigated. Blending of Portland cement with limestone was found to influence the hydrate assemblage of the hydrated cement. Thermodynamic calculations as well as experimental observations indicated that in the presence of limestone, monocarbonate instead of monosulfate was stable. Thermodynamic modelling showed that the stabilisation of monocarbonate in the presence of limestone indirectly stabilised ettringite leading to a corresponding increase of the total volume of the hydrate phase and a decrease of porosity. The measured difference in porosity between the "limestone-free" cement, which contained less than 0.3% CO_2, and a cement containing 4% limestone, however, was much smaller than calculated.

Coupling of thermodynamic modelling with a set of kinetic equations which described the dissolution of the clinker, predicted quantitatively the amount of hydrates. The quantities of ettringite, portlandite and amorphous phase as determined by TGA and XRD agreed well with the calculated amounts of these phases after different periods of time. The findings in this paper show that changes in the bulk composition of hydrating cements can be followed by coupled thermodynamic models. Comparison between experimental and modelled data helps to understand in more detail the dominating processes during cement hydration.

Keywords: Hydration; Limestone; Modelling; Pore solution; Thermodynamic

1. Introduction

Portland–limestone cements are the most widely used cements in Europe. Two classes exist in EN 197-1 designated as CEM II/A-L and CEM II/B-L in which the maximum contents of limestone are 20 and 35% respectively. Besides these special classes, limestone is widely used in all other European common cement types as 0–5% minor additional constituents. The use of up to 5% ground limestone in Portland cement is also permitted by the Canadian cement standard since the early 1980s (CSA 1998 - CAN/CSA-A5) and in more than 25 other countries.

From the point of view of the hardened concrete, up to 5% limestone per mass of cement seems to have little effect on the short and long term macroscopic performance. Regarding mechanical properties, several studies have shown that the compressive strength is more or less the same, or slightly increased, this effect is usually attributed to the fine particle size distribution of the limestone, enhancing the hydration of the clinker by the filler effect, rather than its influence on the chemistry or the packing. The same trend is observed with the flexural strength and the drying shrinkage. As for durability issues, the behaviour of the material with respect to all major aggressive species (sulfates, chlorides, carbonation) and main pathologies (freezing-thawing, ASR, corrosion…) is the same as for limestone free concrete. Neither are the diffusion processes significantly modified: measured oxygen permeability and water sorption are more or less unchanged. Negative effects on the properties discussed above start to be observed when the amount of limestone per mass of cement exceeds 10-15%, such that the drop in the reactive clinker component results in significant physical modifications of the material. A good review on all these aspects can be found in Hawkins et al. [1].

* Corresponding author.
E-mail address: barbara.lothenbach@empa.ch (B. Lothenbach).

0008-8846/$ - see front matter © 2008 Elsevier Ltd. All rights reserved.
doi:10.1016/j.cemconres.2008.01.002

At the low addition level of <5%, some modification of the heat of hydration at early ages may be observed depending on the fineness of the limestone, and the long term heat flow is a bit lower than without limestone due to the smaller fraction of hydrating clinker.

The chemistry associated with the hydration process seems to be the area where the effects of limestone are observed, even at such low levels. Early in the 1990s, several studies showed that limestone seems to favour crystallization of monocarbonate rather than monosulfate [2–4], with the consequence of increasing the amount of ettringite [2]. The high affinity between calcium aluminate and carbonate phases to form monocarbonate had previously been reported by Feldman et al. [5] and Bensted [6]. Some studies therefore looked at the possible substitution of calcium sulfate with limestone. It has been shown that depending on the fineness of the ground clinker and the level of sulfate in the system, calcium sulfate can be replaced up to 25% by calcium carbonate without any modification of the properties of the system [6–8].

In this paper the hydration of two cements was investigated, an OPC containing <0.3% CO_2 intermixed with 0 and 4% of limestone (equivalent to 1.7% CO_2). Thermodynamic modelling has been used to predict the composition of the liquid and solid phase in a hydrating Portland cement in the absence and presence of limestone in the cement.

2. Materials and methods

All experiments were carried out using the same Portland cement with and without limestone. Laboratory ground clinker was homogenized with gypsum (Fluka purum p.a.; previously ground in isopropanol to a mean particle size of 4μm). A part of the cement was blended with 4% of ground natural limestone (mean particle size: 4μm): PC4, while the other part was used without limestone addition (PC). The chemical compositions of the materials as given in Table 1 were determined by X-ray fluorescence (XRF), sulfur and carbonate with a LECO C/S analyzer, and free lime according to Franke [9]. The mineralogical composition was calculated by X-ray Diffraction (XRD)/Rietveld analysis.

The distribution of the alkalis between sulfates and oxides in the unhydrated cement was determined based on the measured concentration of the readily soluble alkalis in bi-distilled water at w/c of 10 after an equilibration time of 5min. These readily soluble alkalis are assumed to correspond to the alkali sulfates present in the clinker, while the remaining K, Na, Mg and S are considered to be associated as minor constituents in solid solution with the major clinker phases [10,11] (cf. Table 1).

A series of cement pastes was prepared at a w/c of 0.4. Calorimetric measurements (Thermometric TAM Air) were carried out with 5g of fresh paste. For the short-term hydration experiments, i.e. up to 6h, small samples of ~ 100g were prepared in the glove box under a N_2-atmosphere. The pore solutions were collected by vacuum filtration using 0.45μm nylon filters. For longer hydration times, larger samples consisting of 1kg cement and 0.4kg water were mixed twice for 90s according to EN 196-3, again prepared in the glove box under a N_2-atmosphere. The pastes were cast in 0.5l PE-bottles, sealed (to exclude the ingress of CO_2) and stored at 20°C. Pore fluids of the hardened samples were extracted using the steel die method and pressures up to 530N/mm^2. The solutions were immediately filtered using 0.45μm nylon filters; after filtration one part was diluted by a factor of 10 with HNO_3 (6.5%) to prevent the precipitation of solid phases, while the rest was used for pH measurements. The pH electrode had been calibrated against KOH solutions of known concentrations. The total concentrations of the elements analyzed were determined using inductively plasma optical emission spectroscopy (ICP–OES).

For TGA analysis, the solid fractions of the samples were crushed, washed in acetone, and dried at 40°C. TGA/DTG was carried out in open vessels in helium on about 10mg of powdered cement paste at 20°C/min up to 980°C. The amount of pore solution in the hardened samples was estimated from the

Table 1
Composition of the cement and the limestone used

	PC	Limestone
Chemical analysis [g/100 g] [a]		
CaO	63.9	55.0
SiO_2	20.2	0.8
Al_2O_3	4.9	0.3
Fe_2O_3	3.2	0.3
CaO (free)	0.93	<0.01
MgO	1.8	1.8
K_2O	0.78	<0.01
Na_2O	0.42	<0.01
CO_2	0.26	42.5
SO_3	2.29	0.05
$K_2O_{soluble}$ [b]	0.72	n.d.
$Na_2O_{soluble}$ [b]	0.09	n.d.
Ignition loss	0.37	43.4
	PC	PC4
Normative phase composition [g/100 g]		
Alite [c]	66.5	64.6
Belite [c]	10.3	9.3
Aluminate [c]	7.5	7.4
Ferrite [c]	8.5	7.8
MgO(periclase) [c]	0.9	0.9
CaO (free) [d]	0.93	0.89
$CaCO_3$ [d]	0.6	4.6
$CaSO_4 \cdot 2H_2O$ [d]	3.1	3.0
K_2SO_4 [b]	1.3	1.3
Na_2SO_4 [b]	0.21	0.20
Present as solid solution in the clinker phases		
K_2O [d]	0.054	0.052
Na_2O [d]	0.33	0.31
MgO [d]	0.94	0.87
SO_3 [d]	0.11	0.11
Blaine surface area [m^2/kg]	413	429
Porosity after 28 days (MIP) vol.% (mortar)	11.99±0.11	11.87±0.01

PC: Portland cement without limestone; PC4: Portland cement blended with 4% limestone.

[a] XRF data corrected for ignition loss.

[b] Readily soluble alkalis calculated from the concentrations of alkalis measured in the solution after 5 min agitation at a w/c of 10; present as alkali sulfates.

[c] From Rietveld analysis, expected errors: phases less than 10 wt.%: +/−0.4%; phases 10–20 wt.%: +/−1%: phases 30 wt.% and more: +/−2%.

[d] Calculated from the chemical analysis.

water loss after exchange with acetone and drying at 40°C; the amount portlandite from the weight loss between 400–520°C. In the presence of no or little C–S–H, i.e. during the first hours of hydration, the weight losses between 50–110°C and 110–140°C were used, respectively, to estimate the amounts of ettringite and gypsum present.

For XRD experiments, cement paste was cast into cylindrical vials. After setting, the paste was kept saturated with water. At the ages 1, 2, 3, 7, 14, 28, 91, 198 and 365days, slices (diameter 3.5cm) were sawn from the cylinder and placed in the diffractometer for XRD pattern acquisition. XRD data were collected using a PANalytical X'Pert Pro MPD diffractometer in a θ–θ- configuration employing CuKα radiation (λ=1.54"Å). The samples were scanned between 7° and 75° with the X'Celerator detector. All Rietveld refinements were done using the X'Pert High Score Plus program from PANalytical. The Rietveld refinement strategy has been previously described in detail by Le Saout et al. [12].

The ^{27}Al NMR spectra were carried out on a Bruker ASX 400 spectrometer (9.4T) at 104.2MHz. ^{27}Al spectra were recorded at 25kHz spinning rate in 2.5mm ZrO_2 rotors. All experiments employed single pulse (π/12) excitation width pulse of 1µs without ^{1}H decoupling and a 0.2s relaxation delay. The ^{27}Al chemical shifts were referenced relative to a 1.0M $AlCl_3$–$6H_2O$ solution at 0ppm.

Mortar prisms were prepared according to EN 196-1. Mortar samples hydrated for 28days were immersed in isopropanol, dried at 50°C and 2–4mm particles were used for the determination of the porosity by mercury intrusion porosimetry (Thermo Fisher Scientific Pascal 440) applying pressures up to 400MPa.

3. Thermodynamic modelling

3.1. Modelling approach

When cement is brought into contact with water, rapidly soluble solids such as gypsum dissolve and come close to equilibrium with the pore solution. The clinker phases hydrate at various rates, continuously releasing Ca, Si, Al, Fe and hydroxide into the solution, which then precipitate as C–S–H, ettringite and other hydrate phases. The dissolution rates of the clinker phases may be considered to determine the amount of Ca, Al, Fe, Si, and hydroxide released into solution and thus to control the precipitation rates of C–S–H, ettringite, and the other hydrates. By combining an empirical model that describes the dissolution of the clinker phases as a function of time [13] with a thermodynamic equilibrium model that assumes equilibrium between the solution and the hydrates, the hydrates formed can be described as a function of time [14]. The model used in this study is described in detail elsewhere [14] and accounts for all the reactions described above. The composition of the solid and liquid phase as a function of time and temperature is calculated based on

i) the composition of the cement paste as given in Table 1,
ii) the calculated degree of the dissolution of the clinkers (see below) and
iii) thermodynamic calculations using a consistent thermodynamic dataset.

The alkalis originating from the dissolution of the alkali sulfates and of the clinker phases distribute between the aqueous solution and the precipitating C–S–H phases. To model the uptake of alkali by C–S–H the same distribution ratio R_d of 0.42ml/g [14,15] was used for both Na and K.

Thermodynamic modelling was carried out using the Gibbs free energy minimization program GEMS [16]. GEMS is a broad-purpose geochemical modelling code which computes equilibrium phase assemblage and speciation in a complex chemical system from its total bulk elemental composition. Chemical interactions involving solids, solid solutions, and aqueous electrolyte are considered simultaneously. The speciation of the dissolved species as well as the kind and amount of solids precipitated are calculated.

The thermodynamic data for aqueous species as well as for many solids were taken from the PSI-GEMS thermodynamic

Table 2
Standard thermodynamic properties at 25 °C

	log K_{S0}[a]	$\Delta_f G°$ [kJ/mol]	$V°$ [cm^3/mol]
(Al–)ettringite	−44.9	−15205.94	707
tricarboaluminate	−46.5	−14565.64	650
Fe–ettringite	−44.0	−14282.36	717
C_3AH_6	−20.84	−5010.09	150
C_3FH_6	−25.16	−4116.29	155
C_4AH_{13}	−25.40	−7326.56	274
C_2AH_8	−13.56	−4812.76	184
$C_4A\bar{S}H_{12}$	−29.26	−7778.50	309
$C_4A\bar{C}H_{11}$	−31.47	−7337.46	262
$C_4A\bar{C}_{0.5}H_{12}$	−29.13	−7335.97	285
C_2ASH_8	−19.70	−5705.15	216
C_4FH_{13}	−29.4	−6430.94	286
C_2FH_8	−17.6	−3917.38	194
$C_4F\bar{S}H_{12}$	−33.2	−6882.55	322
$C_4F\bar{C}H_{12}$	−35.5	−6679.20	290
$C_4F\bar{C}_{0.5}H_{12}$	−33.1	−6440.19	296
C_2FSH_8	−23.7	−4809.53	227
M_4AH_{10}	−56.02	−6394.56	220
M_4AcH_9	−51.14	−6580.15	220
M_4FH_{10}	−60.0	−5498.84[b]	232
$C_{1.67}SH_{2.1}$(jen.)	−13.17	−2480.81	78
$C_{0.83}SH_{1.3}$(tob.)	−8.0	−1744.36	59
Portlandite	−5.20	−897.01	33
$SiO_{2,am}$	1.476	−848.90	29
H_2O	−14.00	−237.18	18
Gypsum	−4.58	−1797.76	75
Anhydrite	−4.36	−1322.12	46
Calcite	−8.48	−1129.18	37
Brucite	−11.16	−832.23	25
$Al(OH)_3$(am)	0.24	−1143.21	32
$Fe(OH)_3$(mic)	−4.60	−711.61	34
C_3S		−2784.33	73
C_2S		−2193.21	52
C_3A		−3382.35	89
C_4AF		−4786.50	130

Thermodynamic data for cements "cemdata2007" taken from Lothenbach et al. [19].
[a]All solubility products refer to the solubility with respect to the species $Al(OH)_4^-$, $Fe(OH)_4^-$, $SiO(OH)_3^-$, OH^-, H_2O, Ca^{2+}, Mg^{2+}, CO_3^{2-} or SO_4^{2-}.

database [17,18]. Solubility products for cement minerals were taken from the recent compilations of Lothenbach et al. [19] and Matschei et al. [20] and are reproduced in Table 2. For modelling the formation of ideal solid solution between Al- and Fe-containing analogues has been assumed [19]. Thus, the expressions ettringite, monocarbonate, monosulfate, hemicarbonate or hydrotalcite in this paper all refer to the solid solution between the Al- and Fe-containing analogues. In should be noted that the recent revision of the thermodynamic database [19,20] indicates that monosulfate is in fact stable with respect to ettringite and hydrogarnet at room temperature and in the presence of water. Thus, whether ettringite or monosulfate is formed just depends on the actual chemical conditions in the respective cement.

3.2. Reactivity of cement clinkers

The hydration of cements can be assumed to take place via a dissolution and precipitation process. The approach of Parrot and Killoh [13], which uses a set of empirical expressions to estimate the degree of dissolution of each clinker mineral as a function of time was used in this paper. This approach describes the rate R of the hydration of the individual clinker phases by a set of equations, where the lowest value of R at time t is considered as the rate-controlling step:

Nucleation and growth $$R_t = \frac{K_1}{N_1}(1-\alpha_t)(-\ln(1-\alpha_t))^{(1-N_1)} \text{ or} \quad (1)$$

diffusion $$R_t = \frac{K_2(1-\alpha_t)^{2/3}}{1-(1-\alpha_t)^{1/3}} \text{ or} \quad (2)$$

Formation of hydration shell $$R_t = K_3(1-\alpha_t)^{N_3}. \quad (3)$$

The degree of hydration α at time t (days) is expressed as $\alpha_t = \alpha_{t-1} + \Delta t \cdot R_{t-1}$. In this paper, the empirical expressions (Eqs. (1)–(3)) as given by Parrot and Killoh [13] are used together with their values of K_1, N_1, K_2, K_3 and N_3 as compiled in Table 3. The influence of the surface area on the initial hydration are included using the data given in Parrot and Killoh [13] as well as the influence of w/c according to $f(w/c) = (1 + 3.333 * (H * w/c - \alpha_t))^4$; for $\alpha_t > H * w/c$. For the critical degree of hydration H, values of 1.8, 1.35, 1.6, and 1.45 were used for alite, belite, aluminate and ferrite, respectively, to obtain a better fit of the data (Figs. 1 and 2).

Table 3
Parameters used to calculate the hydration of the individual clinker phases as a function of time

Parameter[a]	Alite	Belite	Aluminate	Ferrite
K_1	1.5	0.5	1.0	0.37
N_1	0.7	1.0	0.85	0.7
K_2	0.05	0.02[a]	0.04	0.015
K_3	1.1	0.7[a]	1.0	0.4
N_3	3.3	5.0	3.2	3.7
H[a]	1.8[a]	1.35[a]	1.6[a]	1.45[a]

[a] All parameters from Parrot and Killoh [13] for OPC except the values K_2 and K_3 for belite and the critical degree of hydration H which were adapted to obtain a better agreement with the measured dissolution of the clinker minerals.

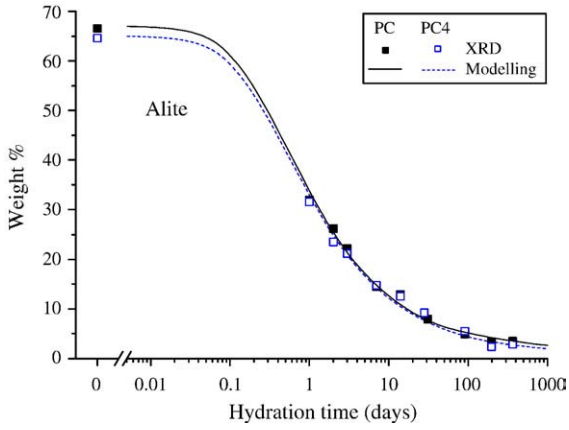

Fig. 1. Amount of alite deduced by XRD/Rietveld analysis as a function of hydration time. Lines are calculated using the adapted cement hydration model of Parrott and Killoh [13].

The Rietveld analysis and TGA give the sum of the phases normalized to 100wt.%. However, the total mass of solids increases with time as hydration products containing water are formed. In the graphs XRD and TGA data are given as measured, and the modelled data were adapted accordingly.

3.3. Changes in solid phases

The modelling indicates that, as the clinkers slowly dissolve as a function of time, different hydrates are formed; initially mainly C–S–H, portlandite and ettringite (Fig. 3). The gypsum present is calculated to be completely depleted within the first 7h of cement hydration. During the first day the calculated hydrate phase concentrations are essentially identical in the systems with and without added limestone.

After a hydration time of 1week or longer, the calculated stable phase assemblages differ strongly in the absence and presence of limestone. In the cement without added limestone, C–S–H, portlandite, monosulfate as well as smaller quantities of hydrotalcite, hemicarbonate and ettringite are predicted to be

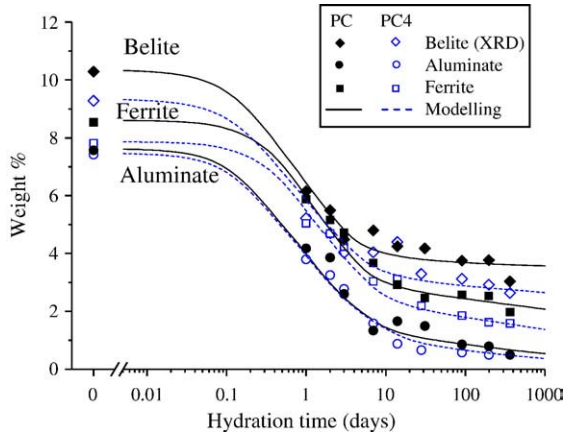

Fig. 2. Amounts of belite, aluminate and ferrite deduced by XRD/Rietveld analysis as a function of hydration time. Lines are calculated using the adapted cement hydration model of Parrott and Killoh [13].

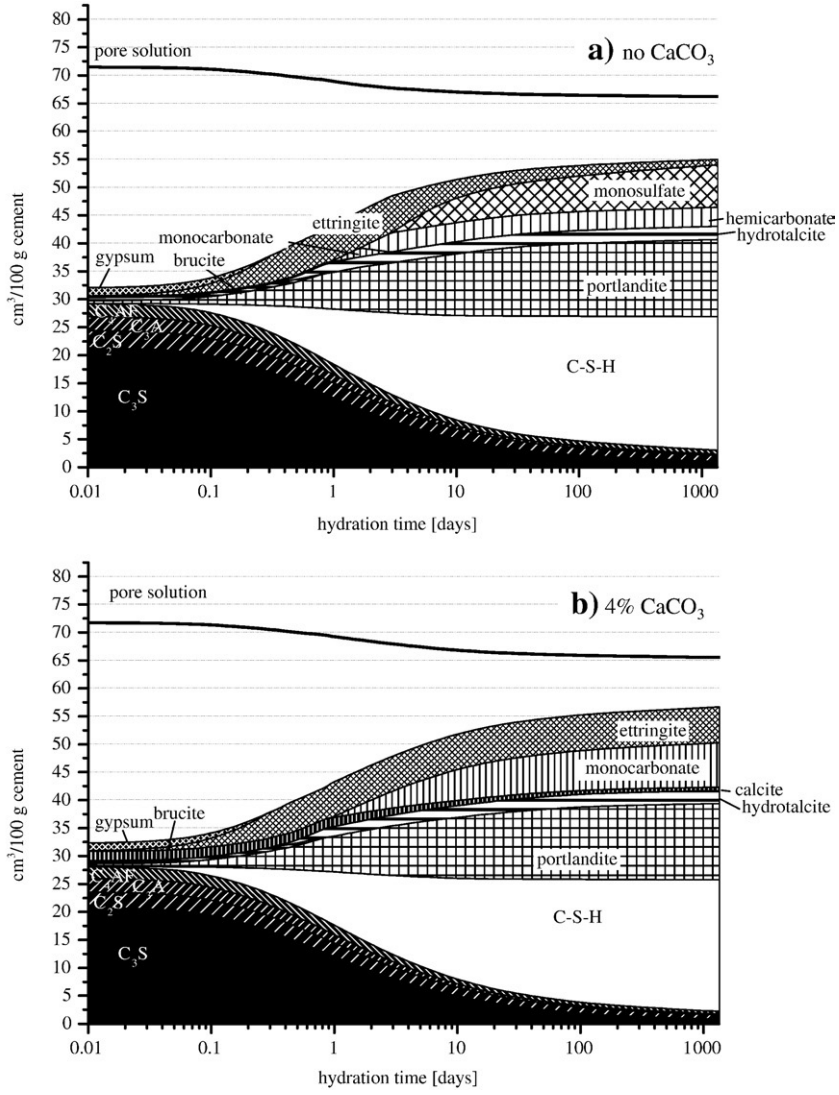

Fig. 3. Modelled changes during the hydration of a) PC, without additional limestone and b) PC4, with 4 wt.% limestone. Volume expressed as cm^3/100 g unhydrated cement.

present. Some hemicarbonate is calculated to form from the small quantity of carbonate present in the clinker. The amount of ettringite is modelled to decrease with time as more and more monosulfate is precipitated. After 1year of hydration approx. 80% less ettringite is predicted for the PC than for the PC4 cement. In PC4, besides C–S–H, portlandite and hydrotalcite, the presence of ettringite, monocarbonate and traces of calcite is predicted. In the presence of limestone significantly more ettringite is calculated as in the presence of limestone monocarbonate and not monosulfate is stable.

The presence or absence of limestone is calculated to affect not only the composition of the hydrate assemblage but also the total volume of the hydrating cement (cf. Fig. 3a and b). The replacement of 4% of the cement by limestone leads to a slightly higher calculated volume after 1week and longer and thus to a slightly lower total porosity. Small amounts of limestone additions (<5%) increase the calculated volume of the solids in hydrated cements at normal hydration temperatures as demonstrated by Matschei et al. [21,22].

3.4. Liquid phase

During the first 6h, the modelled composition of the pore solution is dominated by potassium and sulfate as shown in Fig. 4. Dissolved calcium, hydroxide and sulfate concentrations are determined by the presence of gypsum and portlandite, aluminium concentrations by ettringite and silicate by C–S–H. After the depletion of gypsum, modelled calcium and sulfate concentrations decrease drastically as the calculated pore solutions equilibrate first with C–S–H, portlandite and ettringite, then in addition with hydrotalcite and finally after 1day also with monocarbonate (cf. Fig. 4).

During the first day the calculated composition of the pore solution evolves similarly in the samples with and without additional limestone. Only after more than 1day do the predicted sulfate and aluminium concentrations start to differ significantly from each other. In the presence of additional limestone, ettringite and monocarbonate are calculated to be present which results in lower aluminium and higher sulfate and

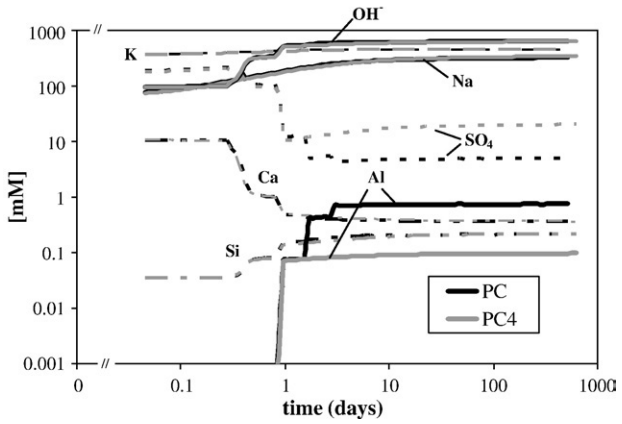

Fig. 4. Modelled concentrations in the pore solution during the hydration of Portland cement without additional limestone (black lines) and blended with 4 wt.% limestone (grey lines).

carbonate concentrations. In the absence of additional limestone the presence of monosulfate instead of monocarbonate leads to higher modelled aluminium and lower sulfate and carbonate concentrations. The calculated concentrations of other ions are not affected by the presence or absence of additional limestone. The concentrations of alkali metal ions in solution, and thus also the pH, are dominated by the dissolution of the clinker phases and the amount C–S–H formed: Ca and Si concentrations are buffered by the presence of portlandite and C–S–H.

4. Experimental results

4.1. Heat evolution

Isothermal conduction calorimetry (Fig. 5) indicates the onset of the acceleration period at approx. 3h in both PC and PC4. The maximal heat evolution was observed for PC4 after 10h and for PC after 11h, indicating a slight acceleration of the cement hydration in the presence of finely ground calcite. This is due to the additional surface provided for the nucleation and growth of hydration products [23,24]. Accordingly, the cumulative heat after 72h expressed per g clinker, is higher for the limestone cement (276J/$g_{clinker}$) than for the PC cement (266J/$g_{clinker}$), again illustrating the accelerating effect of limestone. The total heat flows after 72h, however, were similar (275J/g in the cement sample containing no calcite and 274J/g in the sample with calcite), due to the effect of clinker dilution.

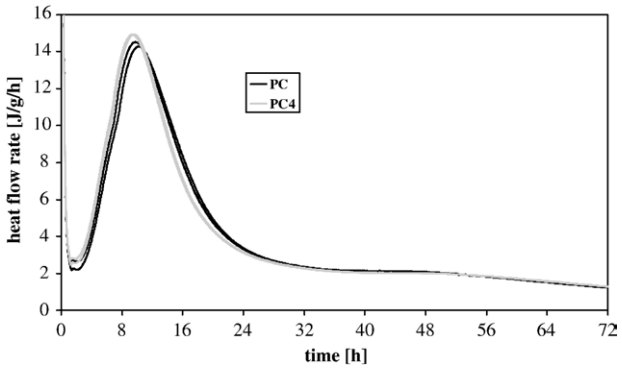

Fig. 5. Isothermal calorimetry of Portland cement without additional limestone PC (black lines) and blended with 4 wt.% limestone PC4 (grey lines) expressed as J/h/g unhydrated cement.

4.2. Solid phases

4.2.1. X-ray diffraction

Fig. 6 shows the XRD pattern of samples PC and PC4 cured for 1year. Anhydrous phases (mainly belite and ferrite) are found in the samples and the presence of calcite in PC4 is still observed after 1year. The main hydration products common to all samples are portlandite, ettringite and ill crystallized C–S–H characterized by the diffuse peak at 2.7–3.3Å (28–33°). The katoite phase was clearly seen as minor phase by XRD after extraction of silicates using salicylic acid in methanol (figure not shown). The term katoite is applied to a solid solution series $Ca_3Al_2Si_3O_{12}$ (grossular) and $Ca_3Al_2(OH)_{12}$ (synthetic phase) with a $SiO_4 \leftrightarrow (OH)_4$ isomorphous replacement and a grossular content of less than 50%. The value of the cell parameter a of the katoite phase (a=1.25nm) seems to indicate a composition close to synthetic phase C_3AH_6 with a possible substitution of Al by Fe [20]. No clear difference in the patterns of katoite in PC and PC4 was found. The main difference between the two XRD patterns at 1year was found in the AFm phases (vertical dotted lines).

In PC, a weak broad peak centred at about 8.5Å (10.4°) appears after 7days (see Fig. 7). This peak decreases in intensity with time and is no longer detected after 91days by which time the monosulfate peak at about 8.97Å is clearly present in the sample. The broad peak at 8.5Å may be assigned to a monosulfoaluminate or hydroxyl-AFm type solid solution [25].

For the blended cement PC4, hemicarbonate (8.2Å) appears at 2days. The peak intensity increases until 14days and then decreases. The characteristic peak of monocarbonate at 7.6Å is detected at 7days and increases with time. As previously noticed

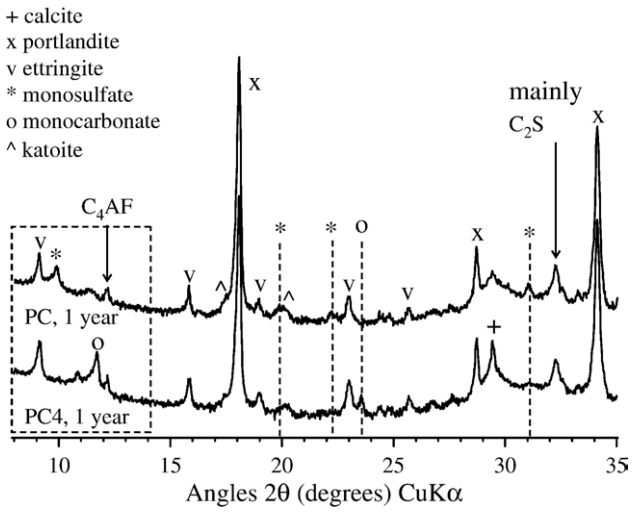

Fig. 6. Observed diffraction pattern for a 1 year hydrated Portland cement without additional limestone (PC) and blended with 4 wt.% limestone (PC4).

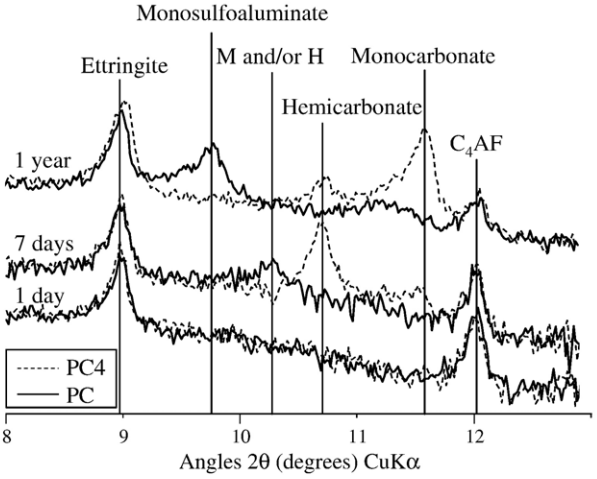

Fig. 7. Observed diffraction pattern between 8 and 13° 2θ degrees (CuKα) for 1, 7 days and 1 year hydrated Portland cement without additional limestone (PC, full line) and blended with 4 wt.% limestone (PC4, dotted line). H: Hydroxy-AFm type solid solution, M: Monosulfate type solid solution.

[25], AFm phases have generally low crystallinity and variations in composition that lead to changes in position and intensity reflections in the XRD patterns. Their quantification by Rietveld analysis is therefore not reliable. Furthermore, the lack of structural data for hemicarbonate impedes its quantification using Rietveld analysis. For this reason, ^{27}Al NMR was also used to investigate the AFt and AFm phases [26] (see section 4.2.3).

4.2.2. Thermogravimetric analysis

The TGA/DTG spectra of the samples hydrated for 400days show similar amounts of hydration products (ettringite, C–S–H, and portlandite) for both PC and the limestone-blended PC4 (Fig. 8). The weight loss at 680°C in PC4 indicates the presence of $CaCO_3$. In addition, a weight loss at approx. 150°C is observed, indicating the presence of monocarbonate. In PC monosulfate (weight loss at approx. 180°C) has formed.

4.2.3. ^{27}Al nuclear magnetic resonance

The ^{27}Al NMR spectra of PC are displayed on Fig. 9. A comparison between PC and PC4 hydrated for about 1year is presented in the upper left corner. The spectra yield signal in the Al(IV) range (100- 40ppm). At 30h, two peaks at about +70 ppm and +82 ppm are observed and attributed to Al for Si substitution in C–S–H and in alite, belite phases, respectively [26]. For hydration times higher than 30h only, the peak at +70 ppm is visible. Upon reaction with water, anhydrous cement forms ettringite and AFm phases which both contain exclusively octahedrally coordinated Al and lead to peaks in the ^{27}Al NMR spectra respectively near +13 and +10ppm. Unfortunately, different AFm phases have almost equal chemical shift and relative strong quadrupolar interactions in comparison with ettringite thus the distinction between the monosulfate, hemicarbonate and monocarbonate is not possible (see [26,27] for ^{27}Al quadrupole coupling and isotropic chemical shift parameters of some AFt and AFm phases). However, NMR spectra clearly show that the AFm content in PC is in the same range of order as the ettringite content whereas the XRD pattern reveals little or no signal of the AFm phase due to its low crystallinity. The resonance at about 5ppm has been attributed by Andersen et al. to an as yet unidentified “Third Aluminate Hydrate” (TAH) [28]. Their work shows that this Al resonance originates from an amorphous or disordered nanoscale aluminate hydrate which is formed either as a separate phase or as a surface precipitate on the C–S–H but not, as previously tentatively assigned, to Al substituting for Ca in the C–S–H layer or interlayer.

4.3. Pore solution

During the first 6h the composition of the pore solutions is dominated by K, S, OH^-, Na, and Ca (cf. Table 4). The concentrations of Ca and sulfate are initially limited by the presence of portlandite ($Ca(OH)_2$) and gypsum ($CaSO_4{\cdot}2H_2O$) in the hydrating cements. The concentration of Al, Si and Fe (they represent beside Ca the major constituents in cement) are always very low. A significant change in the composition of the pore solution takes place between 6 and 24h (Table 4). Ca and sulfate concentrations decrease after the gypsum is depleted due to the formation of ettringite. Hydroxide concentrations increase at the same time in order to maintain charge balance. Al and Si concentrations increase slightly as the pH increases. After the first day, alkali concentrations increase as alkalis continue to be released during the hydration of clinkers and as the volume of the liquid phase present decreases. This steady increase of alkalis leads to a continued increase in pH and thus to a decrease of Ca and an increase of Al, Si and sulfate concentrations (cf. Table 4). The observed trends are consistent with those reported in other studies, e.g. [14,29,30].

Generally, similar concentrations were observed in PC and PC4, with exception of sulfate and aluminium for which respectively higher and lower concentrations were observed in the presence of limestone (cf. Table 4). During the first day, slightly lower concentrations of Na, K, and also of some minor elements such as Li, Cr or Mo are observed in PC4 (vs. PC), presumably because these elements originate from the clinker (of which there is 4% less).

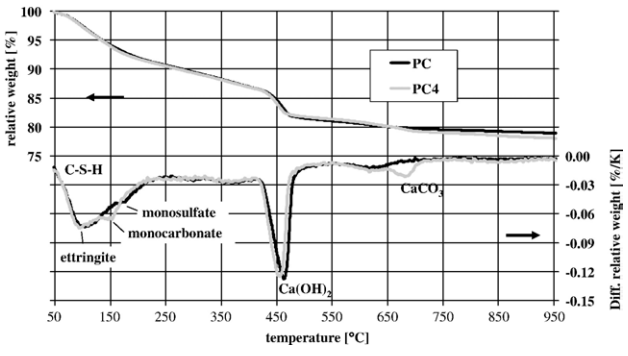

Fig. 8. TGA data of Portland cement without additional limestone samples (PC) and with 4 wt.% limestone (PC4, dotted line) hydrated for 400 days.

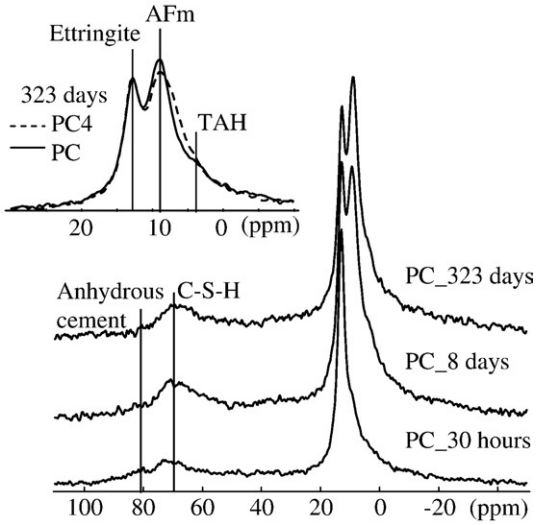

Fig. 9. ^{27}Al MAS NMR spectra of hydrated Portland cement without additional limestone samples (PC) hydrated for 30 h, 8 and 323 days. In the upper left corner, ^{27}Al MAS NMR spectra of hydrated Portland cement without additional limestone samples (PC) and blended with 4 wt.% limestone (PC4, dotted line) hydrated for 323 days.

The charge balance calculated from the measured concentrations indicates an accurate measurement of the composition of the pore solutions during the first 28days (cf. Table 4). After 197 and 400days, however, a surplus of cations of 16% on average is observed. It can be expected that the charge balance is not exact in many cases as both the measurements of alkali with ICP–OES as well as the determination of the hydroxide concentrations by pH measurements can be associated with considerable errors due to inaccuracy of the measurements and possible carbonation in the case of pH measurements. The reason for the relatively large surplus of cations found after 197 and 400days in our samples is not clear, but most probable associated with these inaccuracies. Theoretically the presence of an additional, unaccounted anions could also be the reason. However, no organic admixture has been used in the experiments, measured chloride concentrations are generally in the range of a few mmol/l or lower. Carbonate concentrations are limited by the presence of calcite to a few mmol/l and lower; measured carbonate concentrations have been found to be in the expected range (unpublished data). These concentrations are too low to account for the observed differences. Similarly, the presence of significant concentrations of other anions or cations is not probable [31], as they are present as very minor elements in the cement matrix. The analysis of the pore solutions results often in a minor charge imbalance of a few percent for both short and long hydration times [14,32–35], in some case a higher charge imbalance was observed after longer hydration times [36].

The solutions are slightly oversaturated with respect to portlandite at all times (Fig. 10) and are initially saturated or slightly oversaturated with respect to gypsum. After the first few hours, the gypsum is depleted and the solutions become very undersaturated with respect to gypsum. The saturation index

Table 4
Measured total concentration in the pore solutions gained from Portland cement without limestone (PC) and from Portland cement blended with 4% limestone (PC4)

Time [days]	Na [mmol/l]	K	Li	Ca	Sr	Ba	Al	Si	S	Cr	Mo	OH^{-} [a]	pH	C.B. [b] [%]
PC														
0.04	76	395	0.50	21	0.07	0.006	0.009	0.11	168	0.93	0.028	170	13.2	−2
0.08	77	404	0.52	21	0.08	0.005	0.004	0.13	175	0.98	0.027	160	13.2	−1
0.17	78	401	0.55	21	0.09	0.005	0.015	0.13	176	0.94	0.023	160	13.2	−2
0.25	83	408	0.59	19	0.12	0.006	0.032	0.17	180	0.81	0.016	160	13.2	−2
1	106	447	0.46	2.5	0.02	0.003	0.22	0.31	2.6	0.12	0.003	470	13.6	3
7	173	556	0.82	1.5	0.02	0.002	0.62	0.31	3.4	0.04	0.001	590	13.7	8
28	189	595	0.91	1.4	0.02	0.002	0.38	0.33	10	0.10	0.002	650	13.8	4
197	333	645	1.1	1.3	0.02	0.003	0.37	0.20	21	0.21	0.002	680	13.8	18
400	396	665	1.2	1.2	0.02	0.003	0.33	0.43	22	0.21	0.001	730	13.8	19
PC4, with limestone														
0.04	68	359	0.45	21	0.07	0.005	0.029	0.19	151	0.83	0.025	160	13.2	−2
0.08	71	373	0.47	21	0.07	0.005	0.039	0.21	159	0.86	0.025	160	13.2	−1
0.17	84	433	0.58	16	0.09	0.004	0.015	0.11	191	0.96	0.022	160	13.2	−2
0.25	83	407	0.60	17	0.12	0.006	0.023	0.14	179	0.75	0.014	160	13.2	−2
1	100	404	0.43	2.4	0.02	0.003	0.22	0.27	1.9	0.12	0.003	450	13.6	−2
7	148	483	0.71	1.6	0.02	0.002	0.24	0.26	5.8	0.15	0.002	540	13.7	1
28	172	532	0.84	1.4	0.02	0.002	0.18	0.25	14	0.18	0.001	600	13.8	0
197	297	570	0.98	1.3	0.02	0.003	0.14	0.14	41	0.29	0.001	600	13.7	12
400	331	563	1.0	1.0	0.02	0.001	0.22	0.53	34	0.25	0.001	610	13.8	15
Detection limits														
0.9	0.03	0.03	0.02	0.002	0.0002	0.0003	0.004	0.2	0.001	0.0003	–	–		

The values for OH^- refer to the free concentrations.
The measured concentrations of Fe are below the detection limit of 0.001 mM. [a]The free concentrations of OH^- are calculated from the measured pH values. [b]The charge balance error C.B. is calculated considering that at this high pH approx. 10% of the hydroxide is complexed by dissolved Na and K and thus not captured by pH measurements. The percentages given refer to the surplus of cations (cations-anions), relative to the total charge caused theoretically by cations (i.e. $Na^+ + K^+ + 2Ca^{2+}$).

with respect to a solid is given by $\log(IAP/K_{S0})$, where the ion activity product IAP is calculated from activities derived from the concentrations determined in the solution and K_{S0} signifies the solubility product of the respective solid. A positive saturation index implies oversaturation, a negative value undersaturation with regard to the respective solid. As the use of saturation indices can be misleading when comparing phases which dissociate into a different number of ions, "effective" saturation indices were calculated by dividing the saturation indices by the number of ions participating in the reactions to form the solids. The formation from the dominant ions OH^-, Ca^{2+}, SO_4^{2-}, or $Al(OH)_4^-$ in the solution was considered but not the influence of H_2O; the values for gypsum, portlandite, ettringite or monosulfate were divided by 2, 3, 15 or 11, respectively.

Calculated effective saturation indices with respect to Al–ettringite are initially relatively high (Fig. 10), but decrease after several hours when all gypsum is consumed. The pore solutions are also oversaturated with respect to monosulfoaluminate. Similarly to ettringite, the oversaturation with respect to monosulfoaluminate decreases with time. The oversaturation with respect to gypsum, portlandite and ettringite is identical in both systems. Only the oversaturation with respect to monosulfoaluminate is slightly higher in the limestone-poor PC than in the PC4 which contains 4% calcite (Fig. 10), indicating that the formation of monosulfate is more probable in the absence of calcite.

The observed saturation indices for portlandite, gypsum, ettringite and monosulfate are similar to the values found in other studies [14,29,37]. Although it has often been observed that the pore solutions of aged Portland cement pastes are oversaturated with respect to portlandite, monosulfate and ettringite, e.g. [14,29,36,37], the source of this apparent oversaturation is unknown. In "pure" system, i.e. in synthetic solutions which just contain aluminium, calcium, alkalis, sulfate, and hydroxide, saturation with respect to ettringite is reached within a few days [38]. In the pore solutions of Portland cement systems with a high w/c, where filtration instead of high pressures have been used to gain the pore solutions, the saturation index of portlandite has been observed to approach zero [39,40], indicating saturation, while it remained constantly over saturated in systems with a lower w/c [14,29,36,37]. Whether the apparent oversaturation observed is due to changes caused by the high pressures used to squeeze out the pore solutions or whether kinetic barriers (e.g. caused by high ionic strength [36,41,42]) are responsible is still unclear.

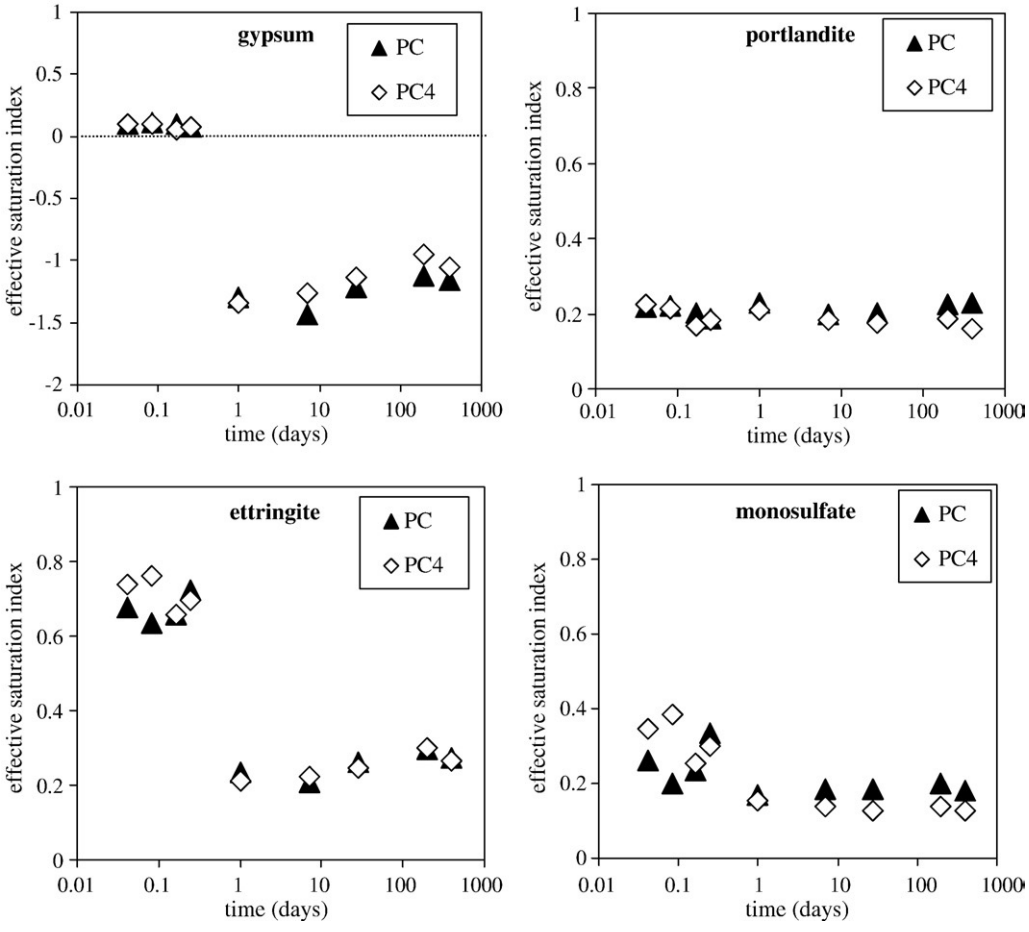

Fig. 10. Effective saturation indices of gypsum, portlandite, ettringite and monosulfate calculated as a function of hydration time. A saturation index of 0 indicates equilibrium between liquid and solid.

5. Discussion

5.1. Modelling and experimental results

Thermodynamic modelling of hydrated limestone blended cement PC4 predicts the presence of C–S–H, portlandite, traces of hydrotalcite, calcite, ettringite and monocarbonate (Fig. 3). In agreement with the calculations, experimentally C–S–H, portlandite, calcite, monocarbonate and ettringite could be identified by XRD and TGA in the hydrated samples.

The amounts of portlandite deduced by XRD and TGA agree well with the calculated quantities (Fig. 11). As previously noticed by comparing NMR and XRD data, the amount of AFm phases deduced by XRD is certainly underestimated due to its low crystallinity and variations in composition which lead to the difference observed in Fig. 12 between measured and calculated AFm phases. Thus it is more appropriate to compare the total amount of amorphous (C–S–H and "amorphous" AFm) and AFm deduced by XRD with the sum C–S–H + AFm of the model as shown in Fig. 13. Besides, a moderate uptake of Al in C-S-H would result in the formation of less AFm and relatively more amorphous C-S-H. In the calculations no uptake of Al in C-S-H has been considered due to the lack of systematic data. The calculated and measured quantities agreed generally very well (Figs. 11 and 12), indicating both the validity of the dissolution model for OPC (cf. Figs. 1 and 2) as well as the ability of thermodynamic equilibrium models to account for the composition of hydrated cement pastes.

In addition, the XRD measurements indicated that initially hemicarbonate has formed, which transformed only very slowly to monocarbonate (cf. Fig. 7). Similarly, Kuzel and Pöllmann [43] observed the early formation of hemicarbonate which later slowly transformed to monocarbonate in a C_3A, lime, gypsum and calcite system. In aqueous systems, hemicarbonate has been found to be unstable in the presence of calcite [44]. Thermodynamic calculations indicate that this should be the same in Portland cement systems. However, the difference in the solubility of hemi- and monocarbonate within the pore solution is rather small. The pore solutions are saturated to a similar degree with respect to both hemi- and monocarbonate and a moderate

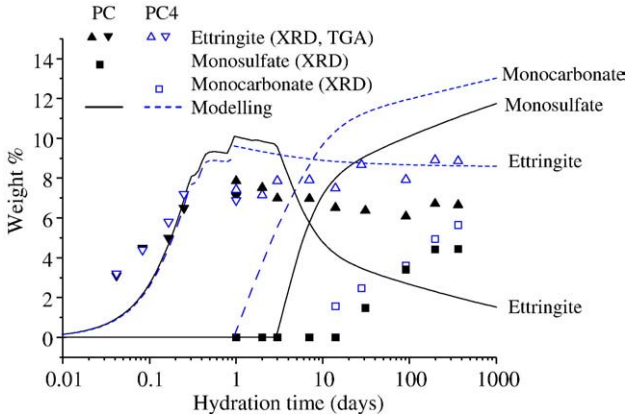

Fig. 12. Amounts of hydrated crystalline products deduced by XRD/ Rietveld analysis as a function of hydration time. Lines refer to the results of thermodynamic modelling.

under saturation with respect to calcite could thus lead to the precipitation of hemicarbonate. No significant difference in the precipitation kinetics between hemi- and monocarboaluminate has been reported [20,45]. While the dissolution of calcite is relatively fast under neutral to moderately alkaline conditions, it slows down significantly above pH 9 [46,47]. Thus, the intermediate formation of hemicarbonate is probably caused by the relatively slow dissolution of limestone, so that initially not sufficient dissolved carbonate is available. However, with time, as more calcite dissolves, hemicarbonate turns into monocarbonate.

For the hydrated PC cement to which no limestone has been added, thermodynamic modelling predicts the formation of C–S–H, portlandite, ettringite, monosulfate and traces of hydrotalcite and hemicarbonate (Fig. 3). In agreement with the calculations, the presence of C–S–H, portlandite and monosulfate could be confirmed by XRD, TGA and NMR measurements. The XRD measurements indicate significantly more ettringite than predicted (Fig. 12). The modelled hydration of PC shows that considerable quantities of ettringite precipitate during the first day, which later should dissolve again and react

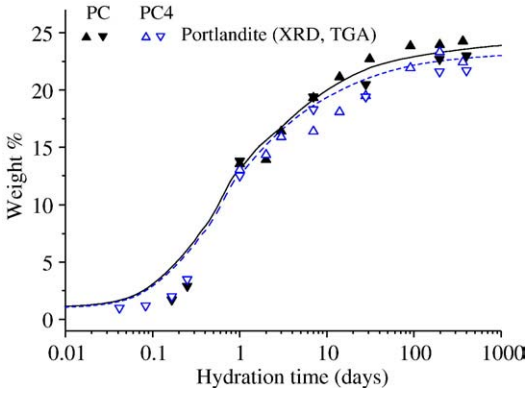

Fig. 11. Amounts of portlandite deduced by XRD/Rietveld analysis and thermal analysis as a function of hydration time. Lines refer to the results of thermodynamic modelling.

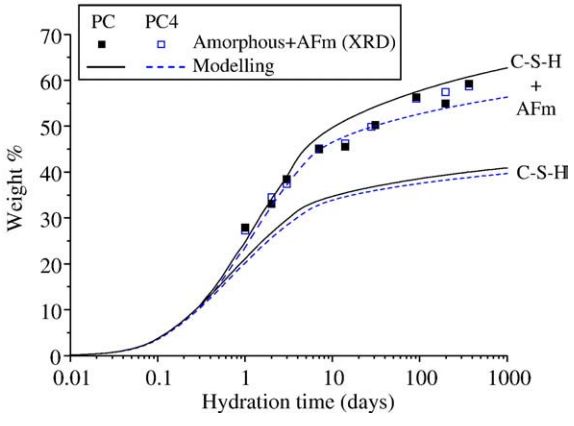

Fig. 13. Amounts of amorphous hydrated products deduced by XRD/ Rietveld analysis as a function of hydration time. Lines refer to the results of thermodynamic modelling.

to form monosulfate. Experimental results confirmed the formation of ettringite during the first day, but most of the ettringite persisted and only a minor fraction dissolved and precipitated as monosulfate. Similar to our observations, Kuzel [48] observed for a cement containing 0.4% CO_2 a slight decrease of ettringite and the formation of some monosulfate after the first day. In contrast, for a cement containing less than 0.1% CO_2 they observed complete disappearance of ettringite within 2 days. The consideration of a moderate uptake of Al in C-S-H in the thermodynamic calculations would lead to less calculated monosulfate and more ettringite which would account better for the observed experimental data.

In addition the pore solutions of the two cements investigated are basically saturated with respect to ettringite (Fig. 10), ettringite has no strong driving force to dissolve rapidly, and thus the formation of monosulfate is expected to be slow. Baur et al. [49] found that, under near equilibrium conditions, ettringite and monosulfate would need between 1 to 4years to re-crystallize completely. Besides, concentrations gradients on a microscopic level, which are not visible in the bulk analysis of pore solutions, could locally influence the stable hydrate assemblage.

Both the modelled and the measured concentration in the pore solutions show consistent trends, as illustrated for PC4 in Fig. 14. The calculations and the measurements showed no significant differences in the composition of the pore solution between PC and the limestone blended PC4 were observed except for the aluminium and sulfate concentrations. The modelling and the measurements indicated consistently a higher sulfate concentration in the presence of calcite and a lower aluminium concentration, even though the trends in the measured data were less explicit than in the modelled data (Fig. 14b).

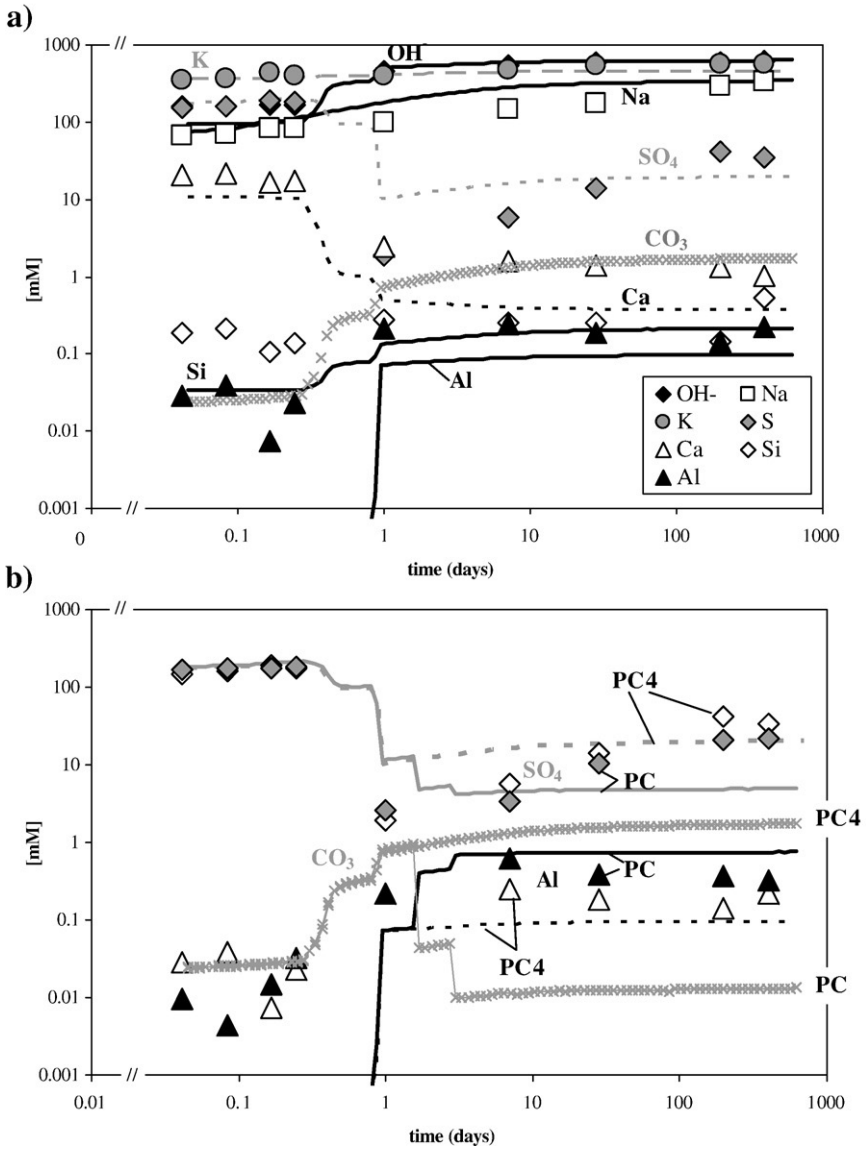

Fig. 14. Modelled concentrations in the liquid phase compared to the experimentally determined concentrations. a) Hydration of PC4 cement, b) aluminium and sulfate concentration in the pore solution of hydrated Portland cement without additional limestone samples (PC) and blended with 4 wt.% limestone (PC4).

5.2. Influence of limestone

The presence of limestone is found to enable the formation of monocarbonate and thus to stabilise indirectly ettringite at the expense of monosulfate. This agrees with other experimental findings: the stabilizing effect of calcite on ettringite has been observed in C_3A, CaO, gypsum and calcite systems [43,50] as well as in calcite-containing Portland cements [48,51,52].

This stabilisation of ettringite in the presence of calcite should lead to an increase of the total volume of the solid phases, as ettringite has a low density and thus a relatively large volume per formula unit (cf. Table 2). In contrast, a reduction in the volume of the hydrated phases should be observed in the absence of limestone. These differences in volume, as illustrated in Fig. 3, should lead to a differences in porosity and thus result in corresponding changes in compressive strength. For the cement investigated, the absence of limestone led after 28days to a calculated lower volume of the hydrate assemblage of approx. 3%. This translates into a relatively moderate calculated difference of the porosity in mortar samples of approx. 0.5vol. %. The measured differences in porosity (see Table 1) were even smaller (≤ 0.1 vol.%). In the investigated "limestone-free" cement much less transformation of ettringite into monosulfate was observed (Fig. 11) than calculated, which accounts for the much smaller difference in porosity. Similar to our observations, different authors reported a small decrease of the porosity if only a few percent (≤ 5%) of the cement was replaced by limestone [52–54]. At higher additions of limestone the dilution effect of the limestone dominates. A small increase in the 28-day compressive strength was observed by some authors [21,53,55], while for other cements [54,56] a small decrease was observed even if only ≤ 5% of the cement was replaced by limestone. Higher additions of limestone led always to a decrease of compressive strength and an increase of porosity, e.g. [53,54,56].

Another effect of the replacement of a fraction of the cement by finely ground limestone is the acceleration of the hydration reaction as shown by calorimetry (Fig. 5). Finely ground limestone accelerates cement hydration as it provides additional surface for the nucleation and growth of hydration products [23,24].

6. Conclusions

Blending of Portland cement with limestone was found to not only accelerate the initial hydration reaction but also to influence the hydrate assemblage of the hydrating cement pastes. Both thermodynamic calculations and experimental observations indicate that in presence of limestone monocarbonate instead of monosulfate is stable at room temperatures.

hermodynamic modelling shows that the stabilisation of monocarbonate indirectly also stabilises ettringite. This is calculated to lead to a corresponding decrease of the total volume of the hydrate phase and an increase of porosity. However, the measured difference in porosity between the "limestone-free" cement, which contained <0.3% CO_2, and the cement containing 4% limestone, was much smaller than calculated. This could be due to an overestimation of the amount of AFm phases in the calculations as no uptake of Al in C-S-H has been considered and/or due to the slow reactivity of ettringite. These findings indicate that Al-uptake in C-S-H could play an important role in Portland cement systems.

The coupling of thermodynamic modelling with a set of kinetic equations which describe the dissolution of the clinker predicts quantitatively the amount of hydrates formed as a function of hydration time. Apart from the minor discrepancies discussed above, the quantities of ettringite, portlandite and amorphous phase as determined by TGA and XRD agreed reasonably well with the calculated quantities of these phases after different periods of time. This illustrates that for the prediction of the bulk evolution of hydrating cements the use of such coupled models can be a valuable tool.

Acknowledgements

The authors would like to thank Holcim Group Support for the supply of clinker and limestone samples. Thanks are extended to G. Möschner (Empa) and H. Mönch (EAWAG) for support during the experiments and for the analysis of the solutions, to J. Kaufmann for the MIP and to D. Rentsch (Empa) for NMR measurements.

References

[1] P. Hawkins, P. Tennis, R. Detwiler, The Use of Limestone in Portland Cement: a State-of-the-Art Review, Portland Cement Association, Skokie, Illinois, USA, 2003.
[2] A.P. Barker, H.P. Cory, The early hydration of limestone-filled cements, in: R.N. Swamy (Ed.), Proc Blended Cements in Construction, Sheffield, UK, Elsevier, 1991, pp. 107–124.
[3] K. Ingram, M. Polusny, K. Daugherty, W. Rowe, Carboaluminate reactions as influenced by limestone additions, in: R.D. Hooton (Ed.), Proc Carbonate Additions to Cement, American Society for Testing and Materials, Philadelphia, PA, 1990, pp. 14–23.
[4] W.A. Klemm, L.D. Adams, An investigation of the formation of carboaluminates, in: P. Klieger, R.D. Hooton (Eds.), Proc Carbonate Additions to Cement, American Society for Testing and Materials, Philadelphia, PA, 1990, pp. 60–72.
[5] R.F. Feldman, V.S. Ramachandran, P.J. Sereda, Influence of $CaCO_3$ on the hydration of $3CaO \cdot Al_2O_3$, J. Am. Ceram. Soc. 48 (1) (1965) 25–30.
[6] J. Bensted, Some hydration investigations involving Portland cement-effect of calcium carbonate substitution of gypsum, World. Cem. Technol. 11 (8) (1980) 395–406.
[7] D.L. Kantro, Calcium carbonate additions, Proc Portland Cement Association - Cement Chemists Seminar, 1978.
[8] V.C. Campiteli, M.C. Florindo, The influence of limestone additions on optimum sulfur trioxide content in Portland cements, in: P. Klieger, R.D. Hooton (Eds.), Proc Carbonate Additions to Cement, American Society for Testing and Materials, Philadelphia, PA, 1990, pp. 30–40.
[9] A. Franke, Bestimmung von Calciumoxid und Calciumhydroxid neben wasserfreiem und wasserhaltigem Calciumsilikat, Z. Anorg. Allg. Chem. 247 (1941) 180–184.
[10] H.W.W. Pollitt, A.W. Brown, The distribution of alkalis in Portland cement clinker, Proc 5th International Congress on the Chemistry of Cement, Tokyo, 1969, October 1986, pp. 322–333.
[11] H.F.W. Taylor, Cement Chemistry, Thomas Telford Publishing, London, 1997.
[12] G. Le Saout, T. Füllmann, V. Kocaba, K.L. Scrivener, Quantitative study of cementitious materials by X-ray diffraction/Rietveld analysis using an

external standard, Proc 12th International Congress on the Chemistry of Cement, Montréal, Canada, July 8-13 2007.
[13] L.J. Parrot, D.C. Killoh, Prediction of cement hydration, Br. Ceram. Proc. 35 (1984) 41–53.
[14] B. Lothenbach, F. Winnefeld, Thermodynamic modelling of the hydration of Portland cement, Cem. Concr. Res. 36 (2) (2006) 209–226.
[15] S.-Y. Hong, F.P. Glasser, Alkali binding in cement pastes. Part I. The C–S–H phase, Cem. Concr. Res. 29 (1999) 1893–1903.
[16] D. Kulik, GEMS-PSI 2.1, 2007, available at http://gems.web.psi.ch/, PSI-Villigen, Switzerland.
[17] T. Thoenen, D. Kulik, Nagra/PSI chemical thermodynamic database 01/01 for the GEM-Selektor (V.2-PSI) geochemical modeling code, PSI, Villigen, 2003, available at http://gems.web.psi.ch/doc/pdf/TM-44-03-04-web.pdf.
[18] W. Hummel, U. Berner, E. Curti, F.J. Pearson, T. Thoenen, Nagra/PSI chemical thermodynamic data base 01/01, Universal Publishers/uPUBLISH.com, USA, also published as Nagra Technical Report NTB 02-16, Wettingen, Switzerland, 2002.
[19] B. Lothenbach, T. Matschei, G. Möschner, F.P. Glasser, Thermodynamic modelling of the effect of temperature on the hydration and porosity of Portland cement, Cem. Concr. Res. 38 (1) (2008) 1–18.
[20] T. Matschei, B. Lothenbach, F.P. Glasser, Thermodynamic properties of Portland cement hydrates in the system $CaO–Al_2O_3–SiO_2–CaSO_4–CaCO_3–H_2O$, Cem. Concr. Res. 37 (10) (2007) 1379–1410.
[21] T. Matschei, D. Herfort, B. Lothenbach, F.P. Glasser, Relationship of cement paste mineralogy to porosity and mechanical properties, Proc Conference on Modelling of Heterogeneous Materials, Prague, June 25-27 2007.
[22] T. Matschei, B. Lothenbach, F.P. Glasser, The role of calcium carbonate in cement hydration, Cem. Concr. Res. 37 (4) (2007) 551–558.
[23] J. Stark, Optimierte Bindemittelsysteme für die Betonindustrie, Beton 54 (10) (2004) 486–490.
[24] J. Pera, S. Husson, B. Guilhot, Influence of finely ground limestone on cement hydration, Cem. Conc. Comp. 21 (2) (1999) 99–105.
[25] T. Matschei, B. Lothenbach, F.P. Glasser, The AFm phase in Portland cement, Cem. Concr. Res. 37 (2) (2007) 118–130.
[26] J. Skibsted, H.J. Jakobsen, Characterization of the calcium silicate and aluminate phases in anhydrous and hydrated Portland cements, in: P. Colombet, A.-R. Grimmer, H. Zanni, P. Soozzani (Eds.), Nuclear Magnetic Resonance Spectroscopy of Cement-Based Materials, Berlin, 1998, pp. 3–45.
[27] P. Faucon, T. Charpentier, D. Bertrandie, A. Nonat, J. Virlet, J.C. Petit, Characterization of calcium aluminate hydrates and related hydrates of cement pastes by 27Al MQ-MAS NMR, Inorg. Chem. 37 (1998) 3726–3733.
[28] M.D. Andersen, H.J. Jakobsen, J. Skibsted, A new aluminium-hydrate species in hydrated Portland cements characterized by 27Al and 29Si MAS NMR spectroscopy, Cem. Concr. Res. 36 (2006) 3–17.
[29] D. Rothstein, J.J. Thomas, B.J. Christensen, H.M. Jennings, Solubility behavior of Ca-, S-, Al-, and Si-bearing solid phases in Portland cement pore solutions as a function of hydration time, Cem. Concr. Res. 32 (10) (2002) 1663–1671.
[30] P. Gunkel, Die Zusammensetzung der flüssigen Phase erstarrender und erhärtender Zemente, Beton-Inf. 23 (1) (1983) 3–8.
[31] A. Goldschmidt, About the hydration theory and the composition of th eliquid phase of Portland cement, Cem. Concr. Res. 12 (1982) 743–746.
[32] F.W. Locher, W. Richartz, S. Sprung, Erstarren von Zement I: Reaktion und Gefügeentwicklung, Zem.-Kalk-Gips 29 (10) (1976) 435–442.
[33] S. Goñi, M.P. Lorenzo, A. Guerrero, M.S. Hernández, Calcium hydroxide saturation factors in the pore solution of hydrated Portland cement fly ash pastes, J. Am. Ceram. Soc. 79 (4) (1996) 1041–1046.
[34] B. Lothenbach, F. Winnefeld, R. Figi, The influence of superplasticizers on the hydration of Portland cement, Proc 12th ICCC, Montreal, Canada, 2007, July 9-12 2007, pp. W1–W5.03.
[35] P. Longuet, L. Burglen, A. Zelwer, La phase liquide du ciment hydraté, Rev. Matér. Constr. 676 (1973) 35–41.
[36] B. Lothenbach, E. Wieland, A thermodynamic approach to the hydration of sulphate-resisting Portland cement, Waste Manage. 26 (7) (2006) 706–719.
[37] J. Stark, B. Möser, F. Bellmann, C. Rössler, Thermodynamische Modellierung der Hydratation von OPC, in: Q.C.d. Zementhydratation (Ed.), Proc 16. Internationale Baustofftagung (ibausil), Weimar, Germany, 20, September 2006, pp. 1–0047–1-0066, -22.
[38] R.B. Perkins, C.D. Palmer, Solubility of ettringite $(Ca_6[Al(OH)_6]_2(SO_4)_3 \cdot 26H_2O)$ at 5–75 °C, Geochim. Cosmochim. Acta 63 (13/14) (1999) 1969–1980.
[39] S.J. Way, A. Shayan, Early hydration of a Portland cement in water and sodium hydroxide solutions: composition of solutions and nature of solid phases, Cem. Concr. Res. 19 (1989) 759–769.
[40] E.M. Gartner, F.J. Tang, S.J. Weiss, Saturation factors for calcium hydroxide and calcium sulfates in fresh Portland cement pastes, J. Am. Ceram. Soc. 68 (12) (1985) 667–673.
[41] M. Michaux, P. Fletcher, B. Vidick, Evolution at early hydration times of the chemical composition of liquid phase of oil-well cement pastes with and without additives. Part I. Additive free cement pastes, Cem. Concr. Res. 19 (1989) 443–456.
[42] W. Ma, P.W. Brown, D. Shi, Solubility of $Ca(OH)_2$ and $CaSO_4 \cdot 2H_2O$ in the liquid paste from hardened cement paste, Cem. Concr. Res. 22 (1992) 531–540.
[43] H.-J. Kuzel, H. Pöllmann, Hydration of C3A in the presence of $Ca(OH)_2$, $CaSO_4 \cdot 2H_2O$ and $CaCO_3$, Cem. Concr. Res. 21 (1991) 885–895.
[44] D. Damidot, F.P. Glasser, Thermodynamic investigation of the $CaO–Al_2O_3–CaSO_4–CaCO_3–H_2O$ closed system at 25 °C and the influence of Na_2O, Adv. Cem. Res. 7 (27) (1995) 129–134.
[45] M.Y. Hobbs, Solubilities and ion exchange properties of solid solutions between OH, Cl and CO3 end members of the monocalcium aluminate hydrates. Thesis University of Waterloo, Ontario, Canada, 2001.
[46] L. Chou, R.M. Garrels, R. Wollast, Comparative study of the kinetics and mechanisms of dissolution of carbonate minerals, Chem. Geol. 78 (1989) 269–282.
[47] W.P. Inskeep, P.R. Bloom, An evaluation of rate equations for calcite precipitation kinetics at pCO_2 less than 0.01atm and pH greater than 8, Geochim. Cosmochim. Acta 49 (1985) 2165–2180.
[48] H.-J. Kuzel, Initial hydration reactions and mechanisms of delayed ettringite formation in Portland cements, Cem. Concr. Compos. 18 (1996) 195–202.
[49] I. Baur, P. Keller, D. Mavrocordatos, B. Wehrli, C.A. Johnson, Dissolution–precipitation behavior of ettringite, monosulfate, and calcium silicate hydrate, Cem. Concr. Res. 34 (2004) 341–348.
[50] H. Kuzel, H. Baier, Hydration of calcium aluminate cements in the presence of calcium carbonate, Eur. J. Mineral. 8 (1996) 129–141.
[51] V.L. Bonavetti, V.F. Rahhal, E.F. Irassar, Studies on the carboaluminate formation in limestone filler-blended cements, Cem. Concr. Res. 31 (2001) 853–859.
[52] T. Schmidt, B. Lothenbach, M. Romer, K.L. Scrivener, D. Rentsch, R. Figi, A thermodynamic and experimental study of the conditions of thaumasite formation, Cem. Concr. Res. 38 (3) (2008) 337–349.
[53] T. Schmidt, Sulfate attack and the role of internal carbonate on the formation of thaumasite. Thesis EPFL, Lausanne, Switzerland, 2007.
[54] S. Tsivilis, J. Tsantilas, G. Kakali, E. Chaniotakis, Sakellariou, The permeability of Portland limestone cement concrete, Cem. Concr. Res. 33 (2003) 1465–1471.
[55] S. Tsivilis, E. Chaniotakis, G. Kakali, G. Batis, An analysis of the properties of Portland limestone cements and concrete, Cem. Concr. Compos. 24 (2002) 371–378.
[56] T. Vuk, V. Tinta, R. Gabrovšek, V. Kaucic, The effects of limestone addition, clinker type and fineness on properties of Portland cement, Cem. Concr. Res. 31 (2001) 135–139.